





Quantitative Susceptibility Mapping of Articular Cartilage in Patients With Osteoarthritis at 3T

Hongjiang Wei, PhD,^{1,2}  Huimin Lin, MD, PhD,³ Le Qin, MD,³ Steven Cao,²
Yuyao Zhang, PhD,^{2,3} Naying He, MD, PhD,⁴ Weibo Chen, PhD,⁵
Fuhua Yan, MD, PhD,^{4*}  and Chunlei Liu, PhD^{2,6*}

Background: Quantitative susceptibility mapping (QSM) has recently been applied in humans to quantify the magnetic susceptibility of collagen fibrils in the articular cartilage.

Purpose: To determine the ability of QSM to detect cartilage matrix degeneration between normal and early knee osteoarthritis (OA) patients.

Study Type: Prospective.

Population: Twenty-four patients with knee OA and 24 age- and sex-matched healthy controls.

Field Strength/Sequence: 3D gradient echo, T₁ turbo spin echo, and proton density-weighted (PDw) spectral attenuated inversion recovery (SPAIR) sequence at 3.0T.

Assessment: Scan–rescan reproducibility of the susceptibility values in the cartilage was assessed in control subjects. Cartilage thickness, volume, mean, and standard deviation (SD) of susceptibility values of the cartilage compartments were compared between normal and OA patients. The relationship between magnetic susceptibility values and cartilage lesion grading based on MR images was studied.

Statistical Tests: The Wilcoxon Rank-Sum test was used to compare cartilage thickness, volume, mean, and SD of susceptibility values between control subjects and OA patients. A Spearman rank correlation was performed to study the relationship between the mean and SD of susceptibility values and the cartilage thinning grades.

Results: The SD of magnetic susceptibility values in the knee cartilage was significantly lower in OA patients compared with healthy controls, and it decreased with more severe MR grades of cartilage thinning degeneration. Significant correlations between the SD of susceptibility values and cartilage thinning grades were observed with $R^2 = 0.64$ and $P = 0.000$, $R^2 = 0.47$ and $P = 0.002$, $R^2 = 0.52$ and $P = 0.001$, $R^2 = 0.42$ and $P = 0.0006$, and $R^2 = 0.67$ and $P = 0.000$ for medial femoral condyle (MFC), lateral femoral condyle (LFC), medial tibia (MT), lateral tibia (LT), and patella, respectively. No significant difference was found in cartilage volume ($P = 0.17$, $P = 0.13$, $P = 0.20$, $P = 0.25$, and $P = 0.18$ for MFC, LFC, MT, LT, and patella, respectively) and thickness ($P = 0.31$, $P = 0.19$, $P = 0.16$, $P = 0.09$, and $P = 0.22$ for MFC, LFC, MT, LT, and patella, respectively) between OA patients and healthy controls.

Data Conclusion: The variations of susceptibility values in the knee cartilage decrease with the degree of cartilage degeneration. QSM may be a sensitive indicator for alteration of the collagen network and shows potential to detect cartilage degeneration at early stage.

Level of Evidence: 2

Technical Efficacy: Stage 3

J. MAGN. RESON. IMAGING 2018.

View this article online at wileyonlinelibrary.com. DOI: 10.1002/jmri.26535

Received Jul 17, 2018, Accepted for publication Sep 14, 2018.

*Address correspondence to: C.L., Department of Electrical Engineering and Computer Sciences, and Helen Wills Neuroscience Institute, University of California, Berkeley, 505 Cory Hall, Berkeley, CA 94720. E-mail: chunlei.liu@berkeley.edu or F.Y., Department of Radiology, Ruijin Hospital, Shanghai Jiao Tong University School of Medicine, No. 197 Ruijin Er Road, Shanghai 200025, China. E-mail: yfh11655@rjh.com.cn

The first two authors contributed equally to this work.

From the ¹Institute for Medical Imaging Technology, School of Biomedical Engineering, MED-X Research Institute, Shanghai Jiao Tong University, Shanghai, P.R. China; ²Department of Electrical Engineering and Computer Sciences, University of California, Berkeley, California, USA; ³School of Information Science and Technology, Shanghaitech University, Shanghai, P.R. China; ⁴Department of Radiology, Rui Jin Hospital, Shanghai Jiao Tong University School of Medicine, Shanghai, P.R. China; ⁵Philips Healthcare, Shanghai, P.R. China; and ⁶Helen Wills Neuroscience Institute, University of California, Berkeley, California, USA

OSTEoarthritis (OA) is a multifactorial degenerative joint disease and is the most common form of arthritis.¹ Characterized by degenerative changes in the cartilage, menisci, ligament, and subchondral bone, OA is considered a disease of the whole joint, and the knee is the most common site affected.² The cartilage thinning and clinical symptoms are preceded by collagen-proteoglycan matrix damage and changes in cartilage water content.³ Therefore, a sensitive technique for detecting these structural changes during the early stages of OA is crucial for improving clinical decision-making, understanding disease progression, and assessing efforts to prevent disease progression.

Magnetic resonance imaging (MRI) is the most accurate noninvasive method available to image and diagnose disorders of the articular cartilage.^{4–6} Various contrast mechanisms corresponding to different MR sequences allow us to probe cartilage physiology and detect changes in cartilage macromolecules, eg, various MR sequences have been used to evaluate cartilage qualitatively^{7,8} and quantitatively.⁹ These advanced MR techniques for detecting cartilage damage include T_2 relaxation, $T_{1\rho}$, ^{23}Na imaging, delayed gadolinium-enhanced MRI of cartilage (dGEMRIC), glycosaminoglycan (GAG) chemical exchange saturation transfer (gagCEST), and diffusion tensor imaging (DTI).^{10–13} In one study, elevated T_2 values were observed in patients with OA.¹⁴ However, this technique is limited by the use of long echo trains, which increase the acquisition time, and the angular dependency of T_2 values on the external magnetic field B_0 makes it difficult to define a “normal” appearance of T_2 maps. In another study, $T_{1\rho}$ values were reported significantly higher in early OA patients compared with healthy subjects⁶; however, $T_{1\rho}$ mapping is limited by its high specific absorption rate and its sensitivity to B_1 inhomogeneity. The dGEMRIC technique has also been used to identify GAG loss in early-stage cartilage disease,¹⁵ but it requires more than an hour of waiting after injection of the contrast agent for effective penetration. gagCEST MRI has also been shown to be a promising technique to quantify GAG content present in the cartilage.¹⁰ Accurate B_0 inhomogeneity estimation is crucial to obtain reliable CEST maps.¹⁶ Lower Na concentration has also been found in the knee cartilage of OA patients using ^{23}Na MRI.¹⁷ However, ^{23}Na MRI is of limited clinical use because of the inherent low sensitivity of sodium signal. Structural imaging techniques such as diffusion-weighted imaging and diffusion tensor imaging (DTI) have been used to measure the water diffusivity restricted by proteoglycan and collagen in the cartilage, and lower fractional anisotropy has been reported in the deep cartilage in patients with OA.¹³ However, DTI’s low spatial resolution and signal-to-noise ratio (SNR), partial volume effects, high sensitivity to motion artifacts, and long acquisition times at clinically relevant field strengths limit its sensitivity and clinical applicability.

Quantitative susceptibility mapping (QSM) is another MRI technique that reflects changes in biochemical composition.¹⁸ In recent years, QSM has been applied in the articular cartilage in animals and humans at ultrahigh field strengths (7T and above). Nissi et al used QSM to improve the visualization of cartilage canals in porcine epiphyseal growth cartilage *ex vivo* and *in vivo*.^{19,20} Yuen et al used T_2^* and frequency maps derived from the multiecho GRE sequence to visualize healthy and abnormal articular cartilage.²¹ Dymerska et al reported that susceptibility-weighted imaging (SWI) and QSM allowed *in vivo* visualization of veins and layers in human growth cartilage.²² Wei et al demonstrated the feasibility of QSM for quantifying the magnetic susceptibility of collagen fibers at different depths in the articular cartilage.²³ A more recent study touched on the quantification of the susceptibility anisotropy of collagen fibrils in the articular cartilage in a porcine *ex vivo* model that was scanned at multiple orientations relative to the B_0 field.²⁴ However, the clinical utility of magnetic susceptibility to differentiate the normal and abnormal cartilage of patients with OA *in vivo* has not been reported.

The aim of this study was to determine the ability of QSM to detect differences between normal and early OA patients due to cartilage matrix degeneration. OA induces structural changes in the constituents of articular cartilage and causes breakdown of the collagen molecules, altering the structural integrity of the collagen fiber network. It has also been suggested that disruption of the collagen network in the superficial zone of articular cartilage is closely involved in the initiation of OA process.²⁵ Changes in such organized collagenous structures are known to affect QSM contrast.²³ Thus, we hypothesized that the variation in the magnetic susceptibility values of the knee cartilage would be related to the severity of OA.

Materials and Methods

Subjects

The study protocol was reviewed and approved by the Institutional Review Board and written informed consent was obtained from all participants prior to enrollment in the study. Twenty-four patients with clinical OA symptoms and 24 age- and sex-matched healthy volunteers were studied. The exclusion criteria for asymptomatic volunteers were any episodes of continued knee pain in the past 3 years and any history of knee surgery or trauma. The basic characteristics of the subjects are shown in Table 1. All patients with knee OA were diagnosed by two fellowship-trained sports medicine physicians during their routine clinical work-up using standardized criteria that included complaints of chronic knee pain, stiffness for a minimum of 6 months, and the American Knee Society Score (AKSS).²⁶

MR Data Acquisition

All images were acquired with a Philips Ingenia 3T MRI scanner (Best, Netherlands) using a dedicated knee coil. The protocol included five sequences: a sagittal 2D T_1 -weighted turbo spin echo

TABLE 1. Characteristics of Participants

	Non-OA	OA	<i>P</i> value
Age (yrs)	42 ± 14	42 ± 14	1
Gender (M/F)	13/11	13/11	1
Body weight (kg)	73.4 ± 13.4	66.7 ± 10.2	0.33
Height (cm)	174 ± 11	169 ± 9	0.24
Body Mass index (kg/cm ²)	27.9 ± 5.6	25.2 ± 3.2	0.16

Values are mean ± SD. *P* values are from Wilcoxon Rank Sum test.

(TSE) sequence (repetition time / echo time [TR/TE] = 547/20 msec, field of view [FOV] = 16 cm, matrix = 356 × 280, slice thickness = 3 mm, turbo factor = 6, bandwidth = ±290 Hz/pixel), sagittal, coronal, and axial 2D proton density-weighted (PD) spin echo sequences with spectral attenuated inversion recovery (SPAIR) fat suppression (TR/TE = 2800/30 msec, FOV = 16 cm, matrix = 322 × 260, slice thickness = 3 mm, bandwidth = ±277 Hz/pixel), and a sagittal 3D spoiled gradient echo (GRE) sequence to image the cartilage with higher spatial resolution (TR/TE = 20/5.1 msec, flip angle = 15°, FOV = 16 cm, acquired matrix = 324 × 324, reconstructed matrix = 560 × 560, slice thickness = 2 mm, number of slices = 70, bandwidth = ±433 Hz/pixel, SENSE factor = 2, scan time = 3.78 min).

Data Reconstruction and Analysis

For each participant, a Laplacian-based phase unwrapping method was applied to unwrap the GRE phase images, V_SHARP (variable-kernel sophisticated harmonic artifact reduction for phase data) filtering was applied to remove the background phase,²⁷ and magnetic susceptibility maps were calculated using the STAR-QSM (streaking artifacts reduction in QSM) method.^{28,29} Susceptibility values were directly used for comparison without referencing to any selected region of interest (ROI), which essentially sets the susceptibility reference to the mean susceptibility of the whole structure within the FOV.

Cartilage was segmented in sagittal GRE magnitude images. Manual ROI selection was conducted using in-house segmentation software, the STISuite V3.0 (<https://people.eecs.berkeley.edu/~chunlei.liu/software.html>). Five compartments were defined in each subject: patella (P), medial femoral condyle (MFC), lateral femoral condyle (LFC), medial tibia (MT), and lateral tibia (LT). The mean and standard deviation (SD) of susceptibility values of each volumetric ROI were calculated for each compartment. Following segmentation, a medial line was generated in each region of the cartilage. The cartilage thickness was determined by calculating the minimal distance from each point on the medial line to a cartilage boundary.³⁰ The average thickness was calculated for each slice and then averaged for all the slices within each compartment. The cartilage volume was determined by multiplying the total number of

voxels of the cartilage by the volume of each voxel. To account for variation in knee size between subjects, the cartilage volume was normalized by the epicondylar distance³¹ determined from axial PD-weighted images.

The manual segmentation of compartments was conducted twice by two radiologists (L.Q., 10 years of experience, and N.H., 8 years of experience; each rater labeled twice). The reported values of each compartment in this study are the mean values obtained from the two raters.

Clinical Assessment Based on Diagnostic MR images

Morphological joint analysis was performed by a fellowship-trained musculoskeletal radiologist (L.Q., 10 years of experience) who was blinded to whether a subject was an asymptomatic volunteer or a patient with knee OA. The radiologist used the sagittal T₁/TSE and sagittal, coronal, and axial PD-weighted SPAIR images to grade the severity of degeneration. Cartilage thinning was defined in each of the five segmented compartments based on T₁- and PD-weighted images according to previously described MR criteria⁶: 0, no obvious thinning; 1, <50% thinning; 2, >50% thinning; and 3, full thickness loss of the cartilage. Each patient was given an overall thinning grade based on the most severe cartilage lesion in each of the five compartments. The bone marrow edema (BME) pattern was defined as hypointensity in the T₁-weighted images, and the grades were defined as 0, no obvious BME; 1, mild edema with less than 1 cm diameter in the long axis along the femoral-tibial direction; 2, moderate edema with diameter between 1 and 3 cm in the long axis along the femoral-tibial direction; and 3, severe edema with diameter larger than 3 cm in the long axis along the femoral-tibial direction. Osteophytes were graded based on T₁- and PD-weighted images as 0, no obvious osteophytes; 1, mild when they are located in the joint margins and were less than 0.5 cm in diameter; and 2, severe when osteophytes were larger than 0.5 cm in diameter. Each patient was given an overall osteophyte score based on the most severe osteophyte. Finally, the overall score was calculated by adding the overall thinning score, BME score, and overall osteophyte score. Overall knee scores between 1–5 were classified as moderate OA and scores larger than 5 were classified as advanced.

The depth-wise profiles from the femoral to the tibial cartilages were calculated by averaging the susceptibility values within the drawn ROI across three slices (Fig. 3a). Comparison was performed between groups based on the overall total knee as graded in the last column of Table 2 (24 healthy controls, 18 moderate OA with score of 1–5, six advanced OA with score 6–10). The cartilage thickness was normalized for comparison to account for variations between subjects.

To assess interobserver agreement, a second fellowship-trained musculoskeletal radiologist (N.H., 8 years of experience) used the MR images to grade the severity of degeneration in each subject using the same criteria.

Test–Retest Reproducibility of Magnetic Susceptibility

To assess test–retest reproducibility, 16 healthy volunteers were imaged twice. The interval between the two scans was 3 months and 4 days. The coefficient of variation (CV) was calculated as the ratio of the SD to the mean susceptibility value for each compartment. Test–retest reproducibility was calculated as the population root-

TABLE 2. Radiological Findings Based on Structural MR Images

Patient ID	Overall cartilage thinning					Overall cartilage thinning	Osteophytes			Overall osteophytes	BME	Overall total score
	MFC	LFC	MT	LT	P		F-P	F-T	Center			
1	1	0	0	0	1	1	1	1	0	1	0	2
2	1	2	1	0	0	2	1	1	1	1	0	3
3	1	0	1	1	1	1	1	1	0	1	1	3
4	0	1	0	1	0	1	2	0	0	2	2	5
5	0	2	0	1	3	3	1	0	1	1	1	5
6	2	2	0	0	1	2	1	0	1	1	2	5
7	3	1	2	3	2	3	2	0	0	2	1	6
8	0	1	0	2	1	2	1	1	0	1	2	5
9	0	0	1	1	0	1	0	1	1	1	1	3
10	1	1	2	1	2	2	1	0	1	1	0	3
11	0	0	0	0	0	0	0	1	0	1	0	1
12	2	3	3	1	1	3	2	1	0	2	1	6
13	1	2	2	1	3	3	2	0	1	2	0	5
14	0	1	0	1	1	1	1	0	0	1	1	3
15	2	0	1	2	0	2	0	1	1	1	1	4
16	3	0	1	1	2	2	3	1	0	3	3	8
17	2	2	1	0	1	2	2	1	0	2	2	6
18	3	1	2	1	3	3	1	0	0	1	0	4
19	2	3	1	1	2	3	0	1	0	1	1	5
20	2	1	3	2	1	3	2	1	2	2	2	7
21	1	1	0	2	0	2	0	1	2	2	3	7
22	2	1	2	1	1	2	0	1	1	1	1	4
23	0	0	0	0	0	0	1	0	0	1	0	1
24	3	1	1	2	2	3	3	0	1	3	0	6

MFC: medial femoral condyle; LFC: lateral femoral condyle; MT: medial tibia; LT: lateral tibia; P: patella; F-T: femoral-tibial joint; F-P: femoral-patella joint; BME: bone marrow edema.

Cartilage thinning grading: 1, < 50% thinning; 2, > 50% thinning; and 3, full thinning (loss) of cartilage.

Osteophytes were graded based on T1- and PD-weighted images as 0, no obvious osteophytes; 1, mild when they are located in the joint margins and were less than 0.5 cm in diameter; and 2, severe when osteophytes were larger than 0.5 cm in diameter.

Bone marrow edema grading: 0, no obvious BME; 1, mild edema with less than 1 cm diameter in the long axis; 2, moderate edema with diameter between 1 and 3 cm in the long axis; and 3, severe edema with diameter larger than 3 cm in the long axis.

mean-squared average coefficient of variation across the 16 volunteers for compartments, according to the formula: $CV_{RMS} = \sqrt{\sum(CV)^2/n}$, where n is the number of subjects. CV_{RMS} values less than 10% were interpreted as good and values below 5% were considered as very good.³²

Statistical Analysis

The Wilcoxon Rank-Sum test was used to compare cartilage thickness and volume, mean susceptibility values, and SD of susceptibility values in the knee cartilage between control subjects and OA patients for compartments. Spearman rank correlation was

TABLE 3. Cartilage Thickness (in mm, mean \pm SD) and Volume (in cm^3/cm , Normalized by Epicondyle Length) in Each Compartment

Cartilage thickness					
	MFC	LFC	MT	LT	P
Controls	1.53 \pm 0.35	1.60 \pm 0.30	1.26 \pm 0.48	1.68 \pm 0.37	2.13 \pm 0.53
OA patients	1.48 \pm 0.18	1.72 \pm 0.33	1.43 \pm 0.32	1.41 \pm 0.40	2.01 \pm 0.46
<i>P</i> value	0.31	0.19	0.16	0.09	0.22
Cartilage volume					
	MFC	LFC	MT	LT	P
Controls	0.33 \pm 0.08	0.46 \pm 0.15	0.13 \pm 0.04	0.22 \pm 0.05	0.27 \pm 0.13
OA patients	0.27 \pm 0.12	0.42 \pm 0.20	0.11 \pm 0.07	0.20 \pm 0.03	0.24 \pm 0.08
<i>P</i> value	0.17	0.13	0.20	0.25	0.18

MFC: medial femoral condyle; LFC: lateral femoral condyle; MT: medial tibia; LT: lateral tibia; P: patella.

performed to study the relationship between mean susceptibility values and cartilage thickness and volume, and between SD of susceptibility values and cartilage thickness and volume. The kappa statistic³³ was used to measure interobserver agreement between the grades given by the radiologists for the cartilage thinning in each compartment, size of osteophytes, and bone marrow lesions.

Results

Table 2 illustrates the main findings based on structural MR images for all the patients, including the cartilage thinning grade in each compartment, osteophytes in the femoral-tibial joint, femoral-patellar joint, joint center, and BME. Among the 24 patients, 12 patients had more severe cartilage thinning at the medial compartments than at the lateral compartments, six had more severe lesions at the lateral compartments, and six had the same lesion grade at both compartments. Cartilage thinning lesions were classified as grade 0 for two patients, 1 for five patients, 2 for eight patients, and 3 for nine patients.

There was high interobserver agreement between radiologists for the grading of the severity of degeneration. The kappa values were 0.80 (95% confidence interval [CI] of 0.653–0.817) for osteophytes, 0.796 (95% CI of

0.621–0.946) for cartilage thinning, and 0.704 (95% CI of 0.564–0.836) for bone marrow edema size.

There were no significant differences in the average thickness and volume of cartilage in OA and control participants (1.61 \pm 0.25 cm vs. 1.64 \pm 0.31 cm for thickness and 0.28 \pm 0.12 cm^3/cm vs. 0.25 \pm 0.11 cm^3/cm for volume normalized by epicondyle length). Table 3 presents the mean values and SD of the cartilage thickness and volume in each compartment for control participants and OA patients. There were no significant differences in either cartilage thickness ($P = 0.31$, $P = 0.19$, $P = 0.16$, $P = 0.09$, and $P = 0.22$ for MFC, LFC, MT, LT, and P, respectively) or volume ($P = 0.17$, $P = 0.13$, $P = 0.20$, $P = 0.25$, and $P = 0.18$ for MFC, LFC, MT, LT, and P, respectively) between these two groups.

Test–Retest Reproducibility of Magnetic Susceptibility

Test–retest reproducibility of the susceptibility values in the knee cartilage of healthy controls is summarized in Table 4. Regional CV_{RMS} values varied between 5.3% (95% CI of 3.1–6.8%) in the P and 8.7% in the MFC (95% CI of 5.3–9.8%).

TABLE 4. Test–retest Reproducibility of Magnetic Susceptibility in the Knee Cartilage on Healthy Controls

	MFC	LFC	MT	LT	P
CV_{RMS}	8.7 (5.3, 9.8)	8.1 (5.8, 9.3)	6.8 (5.2, 8.1)	7.2 (5.4, 8.5)	5.3 (3.1, 6.8)

Data are percentages, with 95% confidence intervals in parentheses. Reproducibility was the root-mean-square average of the coefficient of variation (σ). MFC: medial femoral condyle; LFC: lateral femoral condyle; MT: medial tibia; LT: lateral tibia; P: patella.

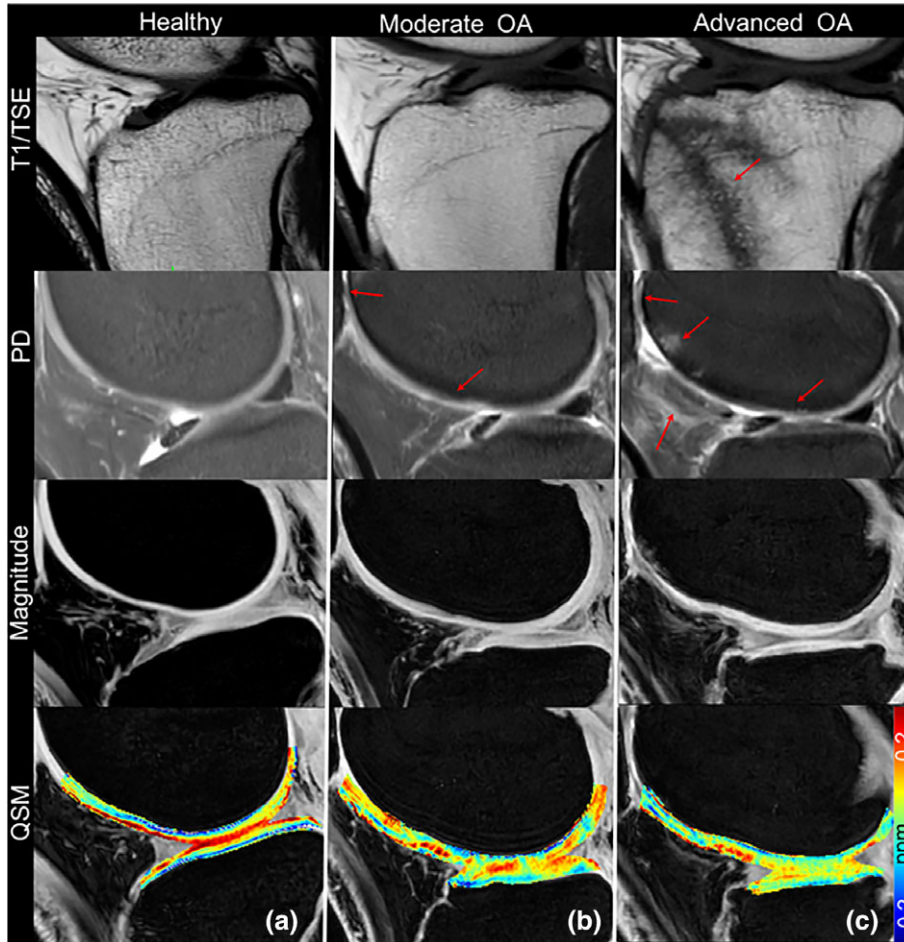


FIGURE 1: Representative T_1 -weighted, Proton density-weighted, 3D GRE magnitude, and QSM images for (a) a healthy control (male, 56 years old); (b) a patient with mild OA (female, 54, patient 18 in Table 2), and (c) a patient with advanced OA (female, 50, patient 16 in Table 2). Cartilage defects and significant osteophytes were seen in patients with mild OA and advanced OA as indicated by the red arrows.

Magnetic Susceptibility Quantification

Figure 1 shows T_1w , PDw, and 3D GRE magnitude images and QSM maps in a healthy control and patients with moderate OA and severe OA. Qualitatively, in the healthy asymptomatic control no cartilage thinning, osteophytes, or other OA symptoms were observed based on the structural images (T_1w , PDw, and GRE magnitude). In the moderate OA patient (patient 18 in Table 2), the minor cartilage thinning and defects were observed as pointed out by the red arrows in Fig. 1b. In the advanced OA patient (patient 16 in Table 2), besides the more severe cartilage thinning (grade 3 in the patella), additional lesions such as osteophytes (grade 3), bone marrow lesions (grade 3), and hyperintensity in the patella fat were observed, as shown in Fig. 1c. As for susceptibility, gradual magnetic susceptibility changes were observed from the superficial layer to the deep layer in the healthy control. Specifically, the susceptibility appears more diamagnetic (colored blue) in the deep layer (-0.076 ppm), relatively less diamagnetic in the middle layer (around 0 ppm), and relatively more paramagnetic in the superficial zone (colored red), referenced to the mean susceptibility of the whole structure, as shown in Fig. 1a and Fig. 2. A dramatic

susceptibility change was observed in knee patients with OA compared with the healthy control in that the multilayer ultrastructure revealed by different magnetic susceptibilities is completely missing (Fig. 1b,c). As shown in Fig. 2b, the distributions of susceptibility values in the cartilage are different for participants with different knee disease stages. More specifically, the spread of the susceptibility distribution of the degraded cartilage in the OA patients is narrower than that of the healthy controls. The variation of susceptibility values decreased as the overall cartilage lesion grades increased. Quantitatively, the mean susceptibility and SD of the whole cartilage were -0.0048 ± 0.12 ppm, -0.01 ± 0.06 ppm, and -0.006 ± 0.038 ppm for the representative healthy control, moderate OA, and advanced OA patients, respectively, as shown in Fig. 2b.

As shown in Fig. 3b, depth-wise susceptibility profiles demonstrated clear differences between healthy controls and OA patients. A decreased susceptibility heterogeneity was observed in the patients with knee OA. For example, the susceptibility values near the cartilage surface of the advanced OA patients (0.032 ppm) was significantly less than those of the healthy controls (0.087 ppm) and patients with moderate OA (0.051 ppm).

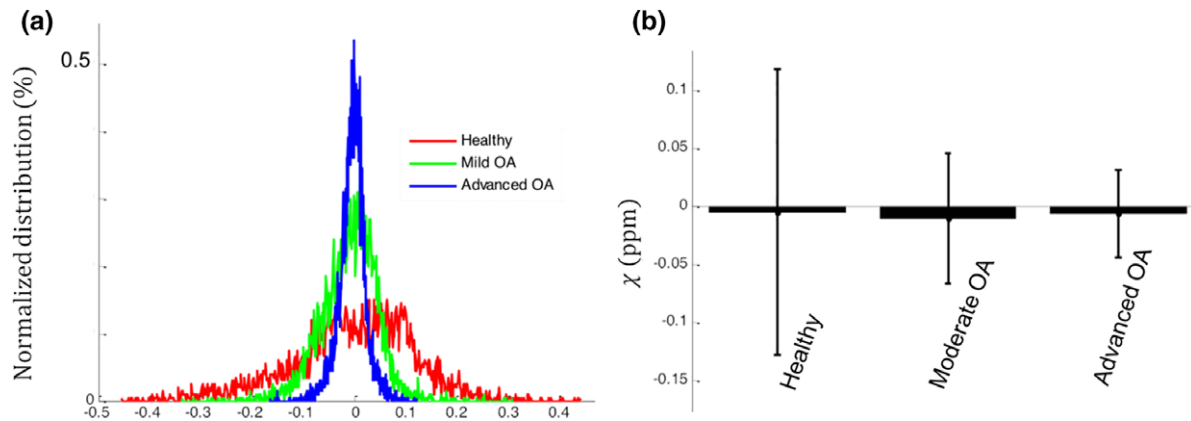


FIGURE 2: Distribution of the magnetic susceptibility values of cartilage on three representative participants as shown in Fig. 1 (a healthy control, moderate OA, and advanced OA refers to patients 18 and 16 in Table 2, respectively). (a) Histograms of the susceptibility of all pixels that were influenced by the grades of cartilage degeneration. The y-axis represents the normalized magnetic susceptibility distribution over the whole 3D cartilage. (b) Mean values and SD of the magnetic susceptibility over the 3D volumetric ROIs from the healthy control and patients with OA as shown in Fig. 1. The susceptibility variation significantly decreases as the overall grades of cartilage lesion increases.

Relationship Between Structural MR Findings and Magnetic Susceptibility Quantification

The mean susceptibility values do not increase as the overall cartilage thinning grade increases from 0 to 3. However, the SD of the susceptibility values decreases as the overall cartilage thinning grade increases from 0 to 3 (from 0.12–0.023 ppm, as presented in Table 5). No significant correlation was found between mean magnetic susceptibility values and cartilage thickness and volume ($P = 0.12$) or between magnetic susceptibility variation and cartilage thickness and volume ($P = 0.19$).

The Spearman correlation between the SD of magnetic susceptibility values and the cartilage thinning grades was also studied for segmented compartments (Table 6). Significant correlations were observed with $R^2 = 0.64$ and $P = 0.000$, $R^2 = 0.47$ and $P = 0.002$, $R^2 = 0.52$ and $P = 0.001$,

$R^2 = 0.42$ and $P = 0.0006$, and $R^2 = 0.67$ and $P = 0.000$ for MFC, LFC, MT, LT, and P, respectively (Fig. 4).

Based on the cartilage thinning grading, we regrouped the 120 compartments for the 24 patients into two groups: mild OA with grades 0 and 1, and advanced OA with grades 2 and 3. No significant difference in mean susceptibility was found between compartments with advanced OA and compartments with mild OA (-0.003 vs. -0.02 , $P = 0.22$). However, the SD of susceptibility values was significantly lower in compartments with advanced OA compared with those with mild OA (0.038 ppm vs. 0.12 ppm, $P = 0.0011$). The percent decrease was 163%.

Furthermore, among the patients with cartilage thinning observed in MR images (grade ≥ 1), 13 patients had “spared” compartments with cartilage thinning grade 0. The SD of susceptibility values for these “spared” compartments

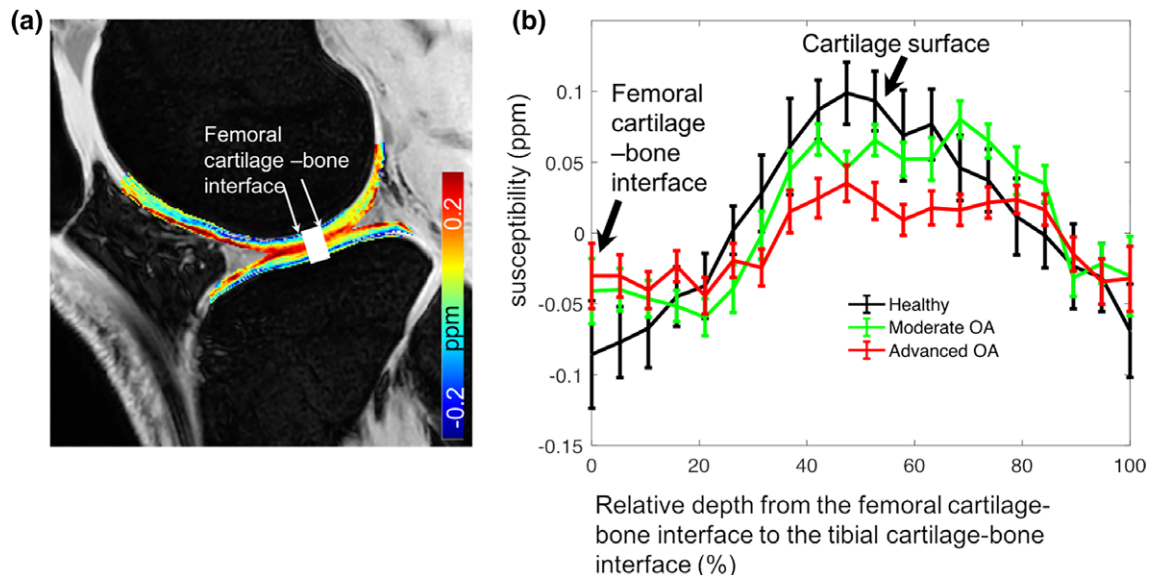


FIGURE 3: (a) The drawn ROI along the femoral to tibial cartilages. (b) The comparison of QSM depth profiles within the ROI between healthy controls and knee OA patients.

TABLE 5. Mean Values and SD of Magnetic Susceptibility in OA Participants vs. Cartilage Overall Thinning Grades Evaluated on MR Images

Cartilage thinning grading	0 (n = 2)	1 (n = 6)	2 (n = 9)	3 (n = 7)
Mean	0.002	-0.04	0.02	-0.003
SD	0.12	0.065	0.032	0.023

was 0.076 ppm, which is lower than that found in the healthy controls (0.14 ppm, $P = 0.01$).

Discussion

This study demonstrated that the variation in magnetic susceptibility values within the knee cartilage was significantly lower in OA patients than in healthy controls. Variation in magnetic susceptibility values also decreased with more severe MR thinning grades of cartilage degeneration.

3D GRE signal phase has proven to be highly sensitive to tissue microstructure alterations. Previous studies

demonstrated the feasibility of using phase and SWI from the 3D multiecho GRE scan to visualize abnormalities of the human articular cartilage.²¹ Phase contrast variation of the veins was observed across the human epiphyseal cartilage.²² Magnetic susceptibility variation was also observed at different depths in the adult cartilage at 7T.²³ In that study, because the accuracy of QSM values in the knee joint was affected by the presence of fat, Wei et al performed water-fat separation to remove the chemical shift. However, this technique increased the scan time: the entire QSM study protocol with shifted echo times could be performed within 17 minutes at a resolution of $0.4 \times 0.4 \times 1.6 \text{ mm}^3$ covering the entire

TABLE 6. Mean Values and SD of Magnetic Susceptibility Values in OA Participants vs. Cartilage Thinning Grades for Compartments

Medial femoral condyle				
Cartilage thinning grading	0 (n = 7)	1 (n = 6)	2 (n = 7)	3 (n = 4)
mean	0.003	0.03	-0.004	0.005
SD	0.11	0.081	0.066	0.042
Lateral femoral condyle				
Cartilage thinning grading	0 (n = 7)	1 (n = 10)	2 (n = 5)	3 (n = 2)
mean	0.01	-0.02	0.003	0.013
SD	0.104	0.071	0.061	0.045
Medial tibia				
Cartilage thinning grading	0 (n = 9)	1 (n = 8)	2 (n = 5)	3 (n = 2)
mean	-0.005	0.023	0.01	0.014
SD	0.102	0.078	0.061	0.037
Lateral tibia				
Cartilage thinning grading	0 (n = 6)	1 (n = 12)	2 (n = 5)	3 (n = 1)
mean	0.003	-0.002	0.005	-0.004
SD	0.113	0.084	0.07	0.045
Patella				
Cartilage thinning grading	0 (n = 7)	1 (n = 9)	2 (n = 5)	3 (n = 3)
mean	-0.002	0.004	0.01	-0.018
SD	0.11	0.082	0.074	0.042

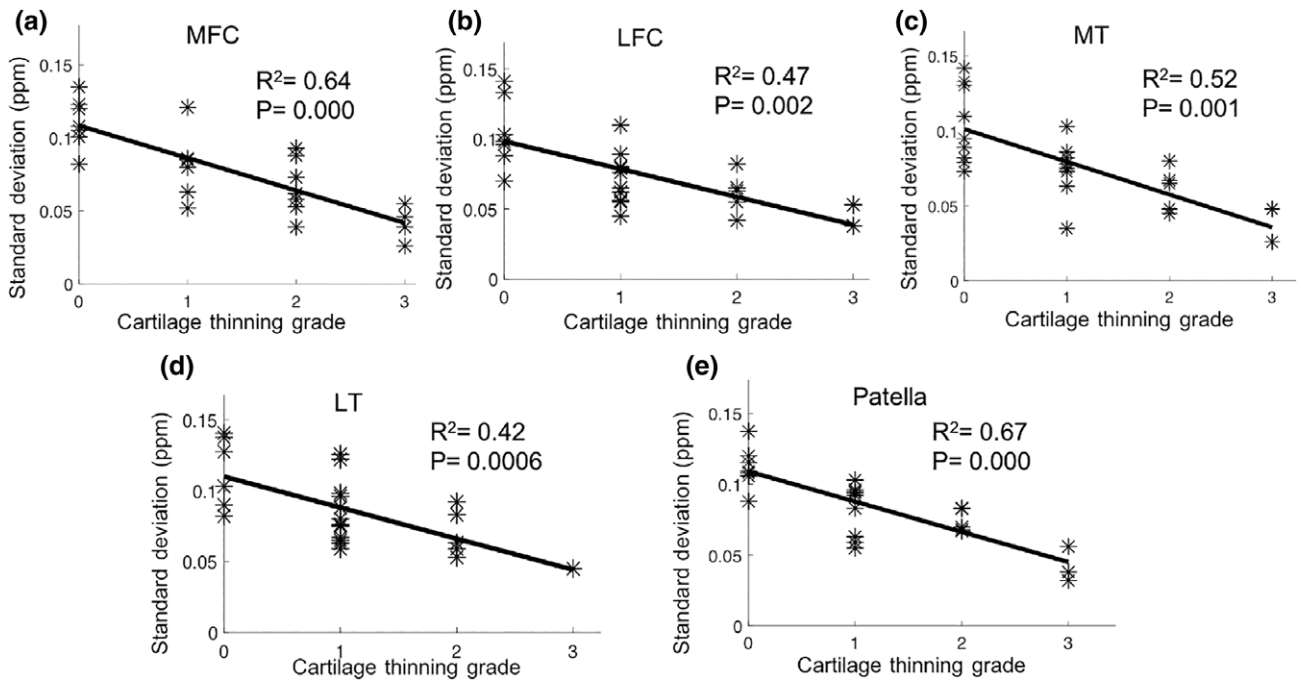


FIGURE 4: Scatterplots and linear regression lines indicate the significant relationships between the SD of magnetic susceptibility values for segmented compartments and cartilage thinning grades. MFC: medial femoral condyle; LFC: lateral femoral condyle; MT: medial tibia; LT: lateral tibia.

knee.²³ In the present study, the single echo 3D spoiled GRE scans were performed with fat saturation at 3T with a scan time of 3.7 minutes at a resolution of $0.28 \times 0.28 \times 2 \text{ mm}^3$. The high in-plane spatial resolution meant that the multilayer ultrastructure revealed by different magnetic susceptibility could be clearly observed in healthy controls, a finding that is similar to the reported values for healthy controls in a previous study.²³ In patients with OA, the missing multiple layer structure was also apparent.

A previous study investigated the feasibility of QSM and T_2^* -mapping for assessing degradation of articular cartilage by measuring ex vivo bovine cartilage samples subjected to different degradative treatments.³⁴ They found that the susceptibility anisotropy of the cartilage differed from the T_2^* anisotropy. However, nonlocal susceptibility effects remain a major difficulty in interpreting GRE. The GRE signal at a location may still have nonzero phase due to the presence of nearby susceptibility sources even if there is no significant susceptibility source in that location. Therefore, T_2^* -mapping is not directly reflective of local tissue properties, especially at ultrahigh-field strengths.

Magnetic susceptibility has the potential to reflect changes in the biochemical composition of cartilage in patients with early OA. Other techniques, including ^{23}Na MRI, dGEMRIC, $T_1\rho$, and T_2 have also shown promising results in imaging cartilage biochemistry. All of these techniques are complementary to standardized cartilage sensitive images and may provide information about changes in proteoglycan or collagen that may exist prior to structural

changes in cartilage thickness. However, these sequences have not been adopted in clinical practice due to a series of limitations and practical challenges.^{7,35} Based on magnetic susceptibility, in healthy controls the observed multiple layer structure due to the magnetic susceptibility anisotropy lies along the collagen long axis.^{23,36,37} The ultra-multilayer structure has been reconstructed using susceptibility tensor imaging (STI) on an ex vivo pig cartilage.²⁴ In diseased cartilage, the missing multiple layers in susceptibility contrast on QSM images indicate microstructure alterations or changes in the constituents of the cartilage. For example, during the early stage of OA, cartilage biochemical and microstructural changes include increased water content, reduced PG concentration, and degradation of matrix macromolecules with disorganization of the collagen network. These changes lead to breakdown and decreased PG content, which in turn lead to ulceration with inflow of PG into the synovial fluid with decreased water content of the cartilage. As OA progresses, collagen, PG, and water content are reduced further and the collagen network becomes severely disrupted.³⁸

We did not compare $R2^*$ and QSM images of OA patients in this study because a previous study showed that the $R2^*$ anisotropy contrast was weaker than the susceptibility anisotropy in the articular cartilage.²³ The explanation is that the $R2$ anisotropy and $R2'$ anisotropy have opposing signs and may cancel each other following the relationship of $R2^* = R2 + R2'$. One previous study on orientation-dependent T_2 relaxation in cartilage showed that the superficial zone has

higher T_2 than the deep zone when the normal specimen surface is parallel to the B_0 field.³⁹ On the other hand, another study showed that T_2' is actually lower in the superficial zone than in the deep zone²³ when the specimen surface is oriented nearly the same relative to the B_0 field. Therefore, the T_2 and T_2' anisotropy cancel each other out, resulting a reduced $R2^*$ contrast between the deep and superficial zone compared with QSM images, as shown in fig. 6 in a previous study.²³

In this study, we did not find a significant difference in cartilage volume and thickness between OA patients and healthy controls. We attribute the lack of volumetric differences to the fact that focal cartilage thinning lesions occurred sparsely in the cartilage, that early OA patients with less structural cartilage loss were examined, and to the varying severity of OA in the diseased group. Furthermore, the cartilage volume and thickness were comparable between OA patients and controls, a finding consistent with previous studies.⁶ These findings indicate that physical measures, such as cartilage thickness, may lag behind biochemical and molecular changes, which can be measured quantitatively with magnetic susceptibility.

The multilayer structural pattern that reveals collagen fibril orientation as observed using magnetic susceptibility has also been verified by the Atomic-Force Microscopy (AFM) experiments in the knee cartilage.²⁴ Other techniques such as polarized light microscopy can also be used to detect the collagen fibril orientation of knee cartilage.³⁴

QSM is valuable in assessing early OA, as it provides specific information on the distribution and content of collagen fibrils in cartilage.³⁴ We are currently investigating the ability of QSM to study the susceptibility changes of knee in aging in a large cohort, as these changes are potentially important to initiate early treatment, monitor disease progression, and follow-up of operative cartilage repair.

Nevertheless, the exact cause of the association between the SD of susceptibility values of the knee cartilage and grade severity remains to be determined. One possible reason is the loss of organization in the collagen fibrils of OA patients. There were indeed regional differences in magnetic susceptibility due to differences in collagen fiber organization,²⁴ which may be degraded in OA. Other possible factors that affect these differences include zonal variations, such as zonal thickness. Future biopsy or ex vivo QSM experiments are needed to determine the exact cause. Combining both in vivo and ex vivo susceptibility information from the same patients may enhance our ability to quantify the cartilage microstructure changes related to OA.

One limitation of this study was that spatial variations of susceptibility values in different cartilage layers were not quantified in the whole knee cartilage, but only in five different compartments. Previous studies developed techniques examining the spatial variation of T_2 within the cartilage and

reported changes in different layers with cartilage degeneration.⁴⁰ It may be helpful to investigate the spatial variation of magnetic susceptibility in different layers of both healthy controls and OA patients to better localize areas of cartilage degeneration. Another limitation was that the present study was a cross-sectional comparison of the differences between OA patients and normal controls with a small number of participants per cohort. Therefore, further work is needed to monitor the changes in magnetic susceptibility during OA disease progression in a longitudinal study, as well as in a larger cohort of OA patients.

Another limitation was that the changes in the magnetic susceptibility values of the articular cartilage were not assessed with histological methods such as polarized light microscopy. In the current study, surgery was not necessary for most of the patients. Therefore, a comparison should be conducted between histological characteristics and the changes of susceptibility values in knee OA patients who will undergo surgical treatment.

In conclusion, QSM allows in vivo imaging and quantification of the magnetic susceptibility of the knee in patients with OA at 3T with a clinically ready protocol and has good scan-rescan reproducibility. Clear susceptibility contrast changes in QSM images were observed in patients with cartilage disease. We demonstrate that the variation of magnetic susceptibility values was significantly lower in OA patients than that of in healthy controls. We also found a correlation between the SD of susceptibility values and the knee disease severity. Therefore, QSM may provide a new way to characterize knee tissue microstructural changes in conjunction with conventional MRI techniques to measure cartilage thickness, volume, and cartilage microstructure.

Acknowledgments

Contract grant sponsor: National Institutes of Health; Contract grant number: NIMH R01MH096979; Contract grant sponsor: ISMRM Research Exchange Program.

References

- Loeser RF, Goldring SR, Scanzello CR, Goldring MB. Osteoarthritis: a disease of the joint as an organ. *Arthritis Rheumatol* 2012;64:1697–1707.
- Oliveria SA, Felson DT, Reed JI, Cirillo PA, Walker AM. Incidence of symptomatic hand, hip, and knee osteoarthritis among patients in a health maintenance organization. *Arthritis Rheumatol* 1995;38:1134–1141.
- Firestein GS, Kelley WN, Budd RC. *Kelley's textbook of rheumatology*. Amsterdam: Elsevier Health Sciences: 2012.
- Nissi MJ, Salo EN, Tiitu V, et al. Multi-parametric MRI characterization of enzymatically degraded articular cartilage. *J Orthop Res* 2016;34:1111–1120.
- Nissi MJ, Lehto LJ, Corum CA, et al. Measurement of T1 relaxation time of osteochondral specimens using VFA-SWIFT. *Magn Reson Med* 2015;74:175–184.

6. Li X, Ma B, Link T. In vivo T1rho and T2 mapping of articular cartilage in osteoarthritis of the knee using 3 Tesla MRI. *Osteoarthritis Cartilage* 2007;15:789–797.
7. Link TM, Stahl R, Woertler K. Cartilage imaging: motivation, techniques, current and future significance. *Eur Radiol* 2007;17:1135–1146.
8. Gold GE, McCauley TR, Gray ML, Disler DG. Special focus session: what's new in cartilage? *Radiographics* 2003;23:1227–1242.
9. Eckstein F, Heudorfer L, Faber S, Burgkart R, Englmeier K-H, Reiser M. Long-term and resegmentation precision of quantitative cartilage MR imaging (qMRI). *Osteoarthritis Cartilage* 2002;10:922–928.
10. Singh A, Haris M, Cai K, et al. Chemical exchange saturation transfer magnetic resonance imaging of human knee cartilage at 3 T and 7 T. *Magn Reson Med* 2012;68:588–594.
11. Hangaard S, Gudbergesen H, Daugaard C, et al. Delayed gadolinium enhanced MRI of menisci and cartilage (DGEMRIM/DGEMRIC) in overweight patients with knee osteoarthritis—a cross sectional study of 86 overweight patients with intraarticular administered gadolinium contrast. *Osteoarthritis Cartilage* 2018;26:S463–S464.
12. Li X, Pedoia V, Kumar D, et al. Cartilage T1ρ and T2 relaxation times: longitudinal reproducibility and variations using different coils, MR systems and sites. *Osteoarthritis Cartilage* 2015;23:2214–2223.
13. Raya JG, Homg A, Dietrich O, et al. Articular cartilage: in vivo diffusion-tensor imaging. *Radiology* 2012;262:550–559.
14. Stahl R, Luke A, Li X, et al. T1rho, T2 and focal knee cartilage abnormalities in physically active and sedentary healthy subjects versus early OA patients—a 3.0-Tesla MRI study. *Eur Radiol* 2009;19:132–143.
15. Tiderius CJ, Olsson LE, Leander P, Ekberg O, Dahlberg L. Delayed gadolinium-enhanced MRI of cartilage (dGEMRIC) in early knee osteoarthritis. *Magn Reson Med* 2003;49:488–492.
16. Krishnamoorthy G, Nanga RPR, Bagga P, Hariharan H, Reddy R. High quality 3D gagCEST imaging of in vivo human knee cartilage at 7T. *Magn Reson Med* 2017;77:1866–1873.
17. Wheaton AJ, Borthakur A, Shapiro EM, et al. Proteoglycan loss in human knee cartilage: quantitation with sodium MR imaging—feasibility study. *Radiology* 2004;231:900–905.
18. Liu C, Li W, Tong KA, Yeom KW, Kuzminski S. Susceptibility-weighted imaging and quantitative susceptibility mapping in the brain. *J Magn Reson Imaging* 2015;42:23–41.
19. Wang L, Nissi MJ, Toth F, et al. Quantitative susceptibility mapping detects abnormalities in cartilage canals in a goat model of preclinical osteochondritis dessicans. *Magn Reson Med* 2017;77:1276–1283.
20. Nissi MJ, Tóth F, Wang L, Carlson CS, Ellermann JM. Improved visualization of cartilage canals using quantitative susceptibility mapping. *PLoS One* 2015;10:e0132167.
21. Yuen J, Hung J, Wiggermann V, et al. Multi-echo GRE imaging of knee cartilage. *J Magn Reson Imaging* 2017;45:1502–1513.
22. Dymerska B, Bohndorf K, Schennach P, Rauscher A, Trattng S, Robinson SD. In vivo phase imaging of human epiphyseal cartilage at 7 T. *Magn Reson Med* 2018;79:2149–2155.
23. Wei H, Dibb R, Decker K, et al. Investigating magnetic susceptibility of human knee joint at 7 Tesla. *Magn Reson Med* 2017;78:1933–1943.
24. Wei H, Gibbs E, Zhao P, et al. Susceptibility tensor imaging and tractography of collagen fibrils in the articular cartilage. *Magn Reson Med* 2017;78:1683–1690.
25. Lotz M, Martel-Pelletier J, Christiansen C, et al. Republished: Value of biomarkers in osteoarthritis: current status and perspectives. *Postgrad Med J* 2014;90:171–178.
26. Martimbianco ALC, Calabrese FR, Iha LAN, Petrilli M, Lira Neto O, Carneiro Filho M. Reliability of the “American Knee Society Score” (AKSS). *Acta Ortoped Brasil* 2012;20:34–38.
27. Wu B, Li W, Guidon A, Liu C. Whole brain susceptibility mapping using compressed sensing. *Magn Reson Med* 2012;67:137–147.
28. Wei H, Zhang Y, Gibbs E, Chen NK, Wang N, Liu C. Joint 2D and 3D phase processing for quantitative susceptibility mapping: application to 2D echo-planar imaging. *NMR Biomed* 2017;30(4).
29. Wei H, Dibb R, Zhou Y, et al. Streaking artifact reduction for quantitative susceptibility mapping of sources with large dynamic range. *NMR Biomed* 2015;28:1294–1303.
30. Solloway S, Hutchinson CE, Waterton JC, Taylor CJ. The use of active shape models for making thickness measurements of articular cartilage from MR images. *Magn Reson Med* 1997;37:943–952.
31. Patel VV, Hall K, Ries M, et al. A three-dimensional MRI analysis of knee kinematics. *J Orthop Res* 2004;22:283–292.
32. Atkinson G, Nevill AM. Statistical methods for assessing measurement error (reliability) in variables relevant to sports medicine. *Sports Med (Auckland, NZ)* 1998;26:217–238.
33. Viera AJ, Garrett JM. Understanding interobserver agreement: the kappa statistic. *Fam Med* 2005;37:360–363.
34. Nykanen O, Rieppo L, Toyras J, et al. Quantitative susceptibility mapping of articular cartilage: ex vivo findings at multiple orientations and following different degradation treatments. *Magn Reson Med* 2018 [Epub ahead of print].
35. Recht M, Bobic V, Burstein D, et al. Magnetic resonance imaging of articular cartilage. *Clin Orthop Relat Res* 2001;391:S379–S396.
36. Worcester DL. Structural origins of diamagnetic anisotropy in proteins. *Proc Natl Acad Sci U S A* 1978;75:5475–5477.
37. Pauling L. Diamagnetic anisotropy of the peptide group. *Proc Natl Acad Sci U S A* 1979;76:2293–2294.
38. Dijkgraaf LC, de Bont LG, Boering G, Liem RS. The structure, biochemistry, and metabolism of osteoarthritic cartilage: a review of the literature. *J Oral Maxillofac Surg* 1995;53:1182–1192.
39. Xia Y, Moody JB, Alhadlaq H. Orientational dependence of T2 relaxation in articular cartilage: A microscopic MRI (μMRI) study. *Magn Reson Med* 2002;48:460–469.
40. Kretzschmar M, Heilmeyer U, Yu A, et al. Longitudinal analysis of cartilage T2 relaxation times and joint degeneration in African American and Caucasian American women over an observation period of 6 years—data from the Osteoarthritis Initiative. *Osteoarthritis Cartilage* 2016;24:1384–1391.